Measurement of $^{17}O(p,\gamma)^{18}F$ between the narrow resonances at $E_r^{lab} = 193$ and 519 keV

J. R. Newton, C. Iliadis, A. E. Champagne, J. M. Cesaratto, S. Daigle, and R. Longland
Department of Physics and Astronomy, University of North Carolina, Chapel Hill, North Carolina, 27599-3255, USA and Triangle Universities Nuclear Laboratory, Durham, North Carolina 27708-0308, USA
(Received 19 October 2009; revised manuscript received 19 November 2009; published 2 April 2010)

The $^{17}O(p,\gamma)^{18}F$ reaction sensitively influences hydrogen burning nucleosynthesis in a number of stellar sites, including classical novae. These thermonuclear explosions, taking place in close binary star systems, produce peak temperatures in the range of $T = 100$–400 MK. Recent results indicate that the thermonuclear rates for this reaction in this particular temperature range are dominated by the direct capture process. We report on the measurement of the $^{17}O(p,\gamma)^{18}F$ cross section between the narrow resonances at $E_r^{lab} = 193$ and 519 keV, where the S factor is expected to vary smoothly with energy. We extract the direct capture contribution from the total cross section and demonstrate that earlier data are inconsistent with our results.

DOI: 10.1103/PhysRevC.81.045801 PACS number(s): 26.30.−k, 24.30.Gd, 25.40.Lw, 26.50.+x

I. INTRODUCTION

Hydrogen burning of ^{17}O sensitively influences nucleosynthesis in a number of stellar sites, including red giants, asymptotic giant branch (AGB) stars, massive stars, and classical novae. The latter phenomenon takes place in a close binary system, where accretion of hydrogen-rich material from a companion star onto the surface of a white dwarf gives rise to a thermonuclear explosion. Peak temperatures during the outburst amount to about $T = 100$–400 MK. For a recent review, see Ref. [1]. The competing $^{17}O(p,\gamma)^{18}F$ ($Q_{p\gamma} = 5606.5 \pm 0.5$ keV) and $^{17}O(p,\alpha)^{14}N$ ($Q_{p\alpha} = 1191.8 \pm 0.1$ keV) reactions at these temperatures are of particular interest in this site since they are important for the galactic synthesis of ^{17}O, the stellar production of radioactive ^{18}F, and for predicted O isotopic ratios in presolar grains. See Ref. [2] for details.

Thus it is not surprising that the $^{17}O + p$ reactions were investigated recently by several groups. The $^{17}O(p,\gamma)^{18}F$ in-beam measurement of Fox *et al.* [2] observed a previously undiscovered resonance at $E_r^{lab} = 193$ keV, which is located inside the energy region (i.e., the Gamow peak [3]) relevant for classical novae. The measured resonance strength,[1] $\omega\gamma_{p\gamma} = (1.2 \pm 0.2) \times 10^{-6}$ eV [2], is a factor of ≈20 smaller than the mean value that was previously estimated by indirect means [4]. Consequently, the $^{17}O(p,\gamma)^{18}F$ thermonuclear reaction rate decreased by an order of magnitude at nova temperatures. This particular resonance was remeasured by the same group in another (p,γ) experiment using a different ^{17}O target, yielding exactly the same value and uncertainty for the strength [5]. Shortly thereafter, two publications by Chafa *et al.* [6,7] reported on properties of the $E_r^{lab} = 193$ keV resonance, corresponding to the state at $E_x = 5789$ keV in ^{18}F. Using an activation method, these authors obtained a resonance strength of $\omega\gamma_{p\gamma} = (3.4 \pm 0.6) \times 10^{-6}$ eV, in disagreement with the earlier results. In addition, Chafa *et al.* observed for the first time the counterpart of this resonance in the competing $^{17}O(p,\alpha)^{14}N$ reaction, reporting a resonance strength of $\omega\gamma_{p\alpha} = (1.6 \pm 0.2) \times 10^{-3}$ eV. It was then discovered [8] that the value for the (p,γ) resonance strength reported by Chafa *et al.* [6] did not account for coincident summing. The corrected value amounted to $\omega\gamma_{p\gamma} = (2.2 \pm 0.4) \times 10^{-6}$ eV [8], still about a factor of 2 larger than the value measured by Fox *et al.* [2,5]. The source of this disagreement is not understood at present. Meanwhile, the (p,α) resonance strength was remeasured independently by two groups, yielding consistent values of $\omega\gamma_{p\alpha} = (1.66 \pm 0.17) \times 10^{-3}$ eV [9] and $\omega\gamma_{p\alpha} = (1.70 \pm 0.15) \times 10^{-3}$ eV [10].

While the discrepancy related to the measured values for the (p,γ) strength of the $E_r^{lab} = 193$ keV resonance clearly needs to be resolved, we would like to address in this work a different, albeit related, problem with the $^{17}O(p,\gamma)^{18}F$ thermonuclear reaction rates, which was first discussed by Fox *et al.* [5]. Consider Fig. 1, showing the level diagram of the ^{18}F compound nucleus near the proton threshold. The three lowest lying resonances occur at $E_r^{lab} = 70$, 193, and 519 keV. For the first resonance, the (p,γ) strength can be estimated reliably from the measured (p,α) and (α,γ) strengths and the α-particle partial width, while the latter two resonances were measured directly [5]. The shaded red bar on the right-hand side shows the energy range ($E_0 = 103$–261 keV) covered by the Gamow peak centroid for nova peak temperatures ($T = 0.1$–0.4 GK). Note that the $E_r^{lab} = 193$ keV resonance ($E_r^{c.m.} = 183$ keV) occurs in the middle of this energy range. Individual contributions to the total (p,γ) reaction rate are displayed in Fig. 2 (adopted from Ref. [5]). Surprisingly, the $E_r^{lab} = 193$ keV resonance is not the dominant contributor to the total reaction rates. This case represents a rare example where a nonresonant process (direct proton capture) dominates the total reaction rates, despite the fact that a narrow resonance is located well inside the Gamow peak [5,7].

The direct proton capture in $^{17}O(p,\gamma)^{18}F$ will be discussed in detail in Sec. II, where it will be pointed out that available

[1]The resonance strength is given in the center-of-mass system and is defined as $\omega\gamma_{px} = (2J+1)(2j_p+1)^{-1}(2j_t+1)^{-1}\Gamma_p\Gamma_x/\Gamma$, with J, j_t, and j_p the spin of resonance, target, and projectile, respectively, and Γ_p, Γ_x, and Γ the proton partial width, γ-ray (or α-particle) partial width and the total width, respectively.

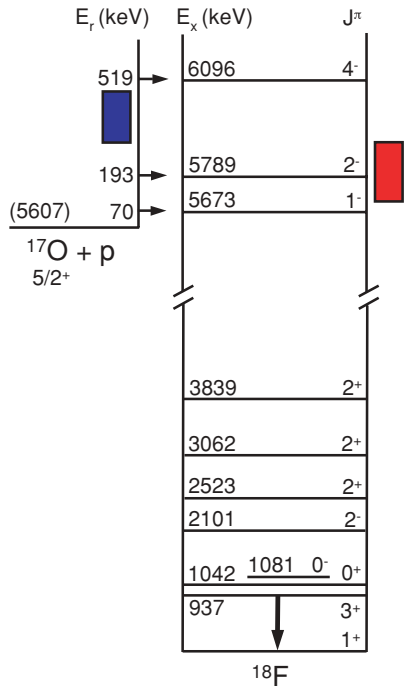

FIG. 1. (Color online) Relevant parts of the energy level diagram for the ^{18}F compound nucleus. Energies and J^{π} values are from Refs. [5,11,12]. The value in parentheses represents the (p,γ) Q value. Resonance energies are given in the laboratory system. Only those bound states are shown from which we observed secondary γ-ray transitions to the ground state. Most of the γ-ray cascades proceed through the first excited state at $E_x = 937$ keV. The red vertical bar on the right-hand side shows the range of Gamow peak centroids for typical nova peak temperatures ($T = 0.1$–0.4 GK, corresponding to $E_0 = 103 - 261$ keV), while the blue vertical bar on the left-hand side indicates the bombarding energy region covered in the present experiment.

data are inconsistent with a straightforward direct capture model calculation, as already noted in Fox *et al.* [5]. In Sec. III we describe a new measurement of the astrophysical S factor at bombarding energies between the narrow resonances at $E_r^{\rm lab} = 193$ and 519 keV (shaded blue bar on the left-hand side of Fig. 1). A new direct capture S factor is presented in Sec. IV and it will become apparent that previous data are inconsistent with the present results. Thermonuclear reaction rates for the ^{17}O$(p,\gamma)^{18}$F reaction are presented in Sec. V. A summary and conclusions are given in Sec. VI.

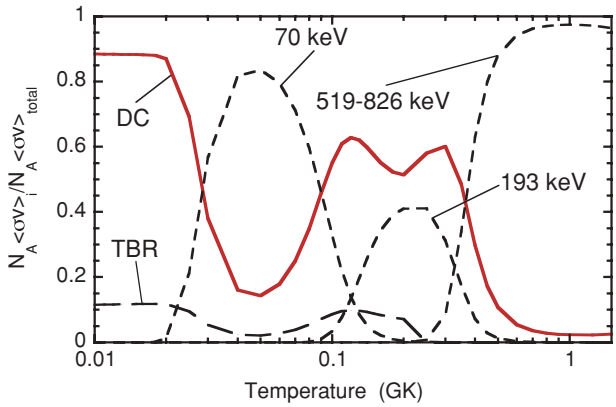

FIG. 2. (Color online) Ratios of individual reaction rate contributions and the total recommended rate [5]. Resonant contributions are labeled by their energy in the laboratory, while contributions from direct capture and the low-energy tails of broad resonances are denoted by "DC" and "TBR", respectively. Direct capture dominates the total reaction rates at nova peak temperatures, $T = 0.1$–0.4 GK.

II. DIRECT PROTON CAPTURE ON ^{17}O

We will first describe how the direct capture contribution, shown in Fig. 2, was estimated in Ref. [5] and subsequently discuss the previously published total cross-section data. Direct proton capture is usually described as a single-step process whereby the proton is directly captured from an initial scattering state into a final bound state with the emission of a γ ray. Contrary to resonant capture, direct capture proceeds without the formation of a compound nucleus. Since capture contributions from the nuclear interior play a less important role for direct capture, the resulting (nonresonant) cross section is expected to vary smoothly with energy. The direct capture cross section can be estimated from the incoherent sum (i) over all orbital angular momenta of the initial scattering state (ℓ_i) and the final state (ℓ_f), and (ii) over all final states j

$$\sigma_{\rm total}^{\rm DC} = \sum_j \sum_{\ell_i \ell_f} C^2 S_j(\ell_f) \sigma_{{\rm calc},j}^{\rm DC}(\ell_i, \ell_f), \qquad (1)$$

with $S(\ell_f)$ and C denoting the single-particle spectroscopic factor and the isospin Clebsch-Gordan coefficient ($C^2 = 1/2$ for $^{17}\mathrm{O} + p \rightarrow {}^{18}$F), respectively. The theoretical direct capture cross section $\sigma_{\rm calc}^{\rm DC}$ for each transition can be calculated, for example, using a single-particle potential model [13]. The cross section for a specific transition to a given final state is determined by the overlap of the scattering wave function in the entrance channel, the bound-state wave function in the exit channel, and the electromagnetic multipole transition operator. The radial wave function for the final bound state can be generated by using a Woods-Saxon potential of suitable shape (radius parameter of $r_0 = 1.25$ fm and diffuseness of $a = 0.65$ fm), where the well depth is chosen to reproduce the experimentally known binding energy of the final state. A hard sphere potential can be adopted for calculating the scattering state radial wave function to disregard capture cross-section contributions from the nuclear interior (which will give rise to resonant capture). Only $E1$ γ-ray transitions need to be taken into account for $^{17}\mathrm{O} + p$ since calculations performed for other multipolarities indicated negligible contributions. For more information and a recent review of this method, see Iliadis and Wiescher [14].

The method outlined previously for estimating the direct capture contribution was applied in numerous calculations of thermonuclear reaction rates and is well established (see, for example, Refs. [14,15]). More sophisticated treatments of calculating the scattering and bound-state wave functions using folding potentials instead of a hard sphere potential and a Woods-Saxon potential give very similar results (see Iliadis *et al.* [16] for a recent analysis of the direct capture in ^{16}O$(p,\gamma)^{17}$F). It must be emphasized that the estimated

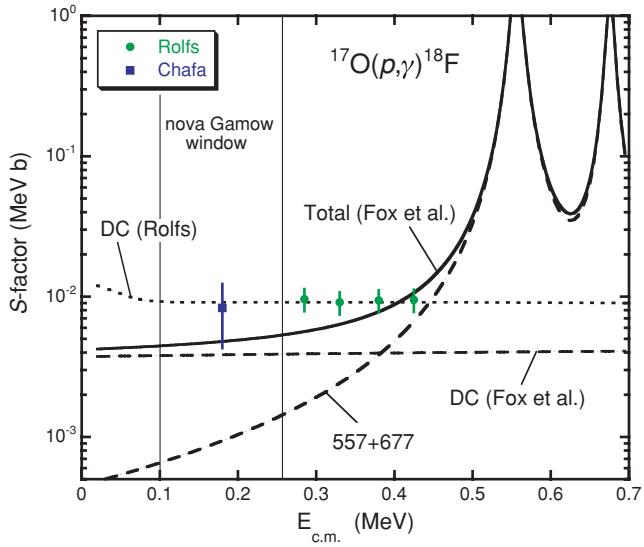

FIG. 3. (Color online) Estimated $^{17}O(p,\gamma)^{18}F$ direct capture S factor from Rolfs [13] (dotted line) and Fox *et al.* [5] (horizontal dashed line). The solid line corresponds to the estimated incoherent sum of resonant capture ($E_r^{\text{c.m.}} = 557$ and 677 keV) and the direct capture contribution from Ref. [5]. The energy range between the two thin vertical lines shows the region of the classical nova Gamow peak centroids (for $T = 0.1$–0.4 GK). Previous S-factor data from Rolfs [13] and Chafa *et al.* [7] are shown as full circles (green) and full square (blue), respectively. The former data points include an 18% uncertainty of the absolute cross-section scale [13]. The two low-energy resonances at $E_r^{\text{lab}} = 194$ and 519 keV are not displayed since they are too narrow to be relevant for the present discussion.

direct capture cross section is not purely based on theory since *experimental* spectroscopic factors are usually employed in Eq. (1). Following this procedure, Fox *et al.* [5] took into account direct capture transitions into 21 final bound states of ^{18}F. Experimental spectroscopic factors were adopted from the $^{17}O(^3He,d)^{18}F$ measurements of Refs. [17,18]. The C^2S values from these two independent studies are mutually consistent. For energies below $E = 1$ MeV, Ref. [5] reported a total $^{17}O(p,\gamma)^{18}F$ direct capture S factor[2] of $S(E_{\text{c.m.}}) \approx 3.7 \times 10^{-3}$ MeVb, with an estimated uncertainty of 50%. The direct capture S factor from Fox *et al.* [5] is shown in Fig. 3 as a dashed (nearly horizontal) line. The S factor from two broad resonances at $E_r^{\text{lab}} = 589$ keV ($E_r^{\text{c.m.}} = 557$ keV, $J^\pi = 3^+$) and $E_r^{\text{lab}} = 716$ keV ($E_r^{\text{c.m.}} = 677$ keV, $J^\pi = 2^+$), calculated using Breit-Wigner amplitudes and experimental resonance parameters from Ref. [11], is also shown as a dashed line.[3] The solid line represents the sum of resonant and direct capture contributions. Between energies of $E_{\text{c.m.}} \approx 200$ and 380 keV the direct capture process is expected to dominate the total S factor.[4]

An alternative, and in some instances preferred, method of estimating the direct capture contribution is a measurement of the total cross section, either directly at energies of astrophysical interest, or at higher energies. In either case it is important to perform the measurement over an extended range of bombarding energies so that the direct capture and resonant capture components can be extracted reliably from the total cross section. Evidently, the larger the resonant contribution to the total cross section, the more difficult the determination of the direct capture amplitude will be. Existing low-energy data prior to this work are shown in Fig. 3. Four data points at center-of-mass energies between $E_{\text{c.m.}} = 280$–425 keV (shown as solid green circles) were reported by Rolfs [13]. Because of the disturbing influence of the broad resonances at $E_r^{\text{c.m.}} = 557$ and 677 keV, Ref. [13] studied the $^{17}O(p,\gamma)^{18}F$ total cross section in detail only above $E = 0.9$ MeV. The higher-energy data were analyzed in terms of Breit-Wigner resonances and a direct capture potential model similar to the one described previously, except that a square-well potential instead of a more realistic Woods-Saxon potential was used for the computation of the bound-state wave function (see the discussion in Ref. [14]). The direct capture contribution derived in the analysis of Rolfs [13] is shown as a dotted line in Fig. 3 and is in agreement with the measured low-energy data points in the $E_{\text{c.m.}} = 280$–425 keV region. Those data points are not otherwise discussed in Ref. [13], other than being displayed in his Fig. 17. However, they clearly correspond in energy to the lowest four data points, shown in his Fig. 11, of the *total* cross section for the $937 \rightarrow 0$ γ-ray transition, which represents the strongest decay branch in ^{18}F. The direct capture model calculation is also shown in Fig. 11 of Ref. [13], indicating that the four low-energy data points are entirely dominated, within uncertainties, by direct capture. This disagrees with the findings of Fox *et al.* [5], who predicted that the higher-lying two data points, at $E_{\text{c.m.}} = 380$ and 425 keV, should be strongly influenced by the broad resonance tails (see previous discussion). Furthermore, a total cross-section measurement using the activation method was reported by Chafa *et al.* [7] at a single, very low, energy of $E_{\text{c.m.}} = 180$ keV, close to the low-energy edge of the $E_r^{\text{c.m.}} = 183$ keV excitation function. This data point is shown as a solid (blue) square in Fig. 3 and seems to agree with the direct capture S factor reported by Rolfs [13]. However, it must be pointed out that its uncertainty amounts to ≈50% and hence the measurement is only of limited significance. In summary, the existing data seem to favor the direct capture S factor reported by Rolfs [13] (dotted line) and disagree with the prediction of Fox *et al.* [5] (dashed horizontal line). The ratio of these two predictions for the direct capture component amounts to a factor of ≈2.5 and has significant consequences for the thermonuclear reaction rates.

[2]The astrophysical S factor is defined by $S(E) = \sigma(E)Ee^{2\pi\eta}$, with σ the cross section and η the Sommerfeld parameter; energies are in the center-of-mass system [3].

[3]These two broad resonances have different J^π values and thus do not interfere in the total S factor; see Sec. IV.

[4]The direct capture process does not interfere with the two broad resonances at $E_r^{\text{lab}} = 589$ and $E_r^{\text{lab}} = 716$ keV since these transitions proceed via different orbital angular momenta ($\ell_i = 1$ and $\ell_r = 0$, respectively); see Sec. IV.

Considering Fig. 3 it may seem strange at first that Fox *et al.* [5] adopted an indirectly estimated direct capture S factor instead of using the prediction of Rolfs [13], which seems to be in agreement with the data at low energy. The reasons were twofold. First, the *energy dependence* of the low-energy data points from Ref. [13] is clearly not consistent with the presence of the two broad resonances at $E_r^{\text{c.m.}} = 557$ and 677 keV. Recall that the resonant contribution, shown in Fig. 3, was calculated in Ref. [5] using experimental resonance parameters [11]. Second, the calculated *energy dependence* of the direct capture cross section from Rolfs (dotted line in Fig. 3; see also Fig. 17 in Ref. [13]) could not be reproduced in Fox *et al.* [5], neither by using a square-well potential for computing the bound-state wave function, as was done in Ref. [13], nor by using a more realistic Woods-Saxon potential. Similar concerns with the low-energy direct capture S factor reported by Rolfs [13] were expressed in Chafa *et al.* [7].

Considering the astrophysical importance of the direct capture in the $^{17}\text{O}(p,\gamma)^{18}\text{F}$ reaction, we undertook a new dedicated measurement of the low-energy cross section at energies between the narrow resonances at $E_r^{\text{lab}} = 193$ and 519 keV.

III. EXPERIMENTAL PROCEDURE

The experiment was carried out at the Laboratory for Experimental Nuclear Astrophysics (LENA), which is part of the Triangle Universities Nuclear Laboratory (TUNL). A 1 MV JN Van de Graaff accelerator supplied proton beams of up to 125 μA on target in the energy range of $E_p^{\text{lab}} = 150$–530 keV. The bombarding energy was calibrated with six well-known resonances in $^{18}\text{O}(p,\gamma)^{19}\text{F}$, $^{26}\text{Mg}(p,\gamma)^{27}\text{Al}$, and $^{27}\text{Al}(p,\gamma)^{28}\text{Si}$ [11,19]. The uncertainty in absolute energy and the energy spread amounted to ± 0.5 and 1.5 keV, respectively. The proton beam entered the target chamber through a liquid-nitrogen cooled copper tube. An electrode was mounted at the end of this tube and was biased to -300 V to suppress the emission of secondary electrons from the target and the beam collimator. The target and chamber formed a Faraday cup for charge integration. The beam was focused into a profile of $\approx$10 mm diameter on target. The target was directly water cooled using deionized water.

Targets of ^{17}O and ^{18}O were prepared by anodizing 0.5 mm thick tantalum backings in ^{17}O- or ^{18}O-enriched water. According to the supplier, the enrichments amounted to 91.2% and 97.5%, respectively. Such targets were found [20] to be of well-defined stoichiometry (Ta_2O_5) with a target thickness that is precisely determined by the anodizing voltage. Prior to target preparation, the surface of the tantalum backing was etched [21] to remove some of the impurities that are a source of beam-induced background radiation. For the ^{17}O and ^{18}O targets, thicknesses of 4.4 ± 0.2 and 32.5 ± 0.5 keV were determined from the measured (p,γ) thick-target excitation functions of the 519 and 151 keV resonances, respectively. A relatively thin ^{17}O target was chosen to simplify the determination of the effective interaction energy of the direct capture cross section (see Sec. IV). The targets were checked frequently and no degradation in the total number of target nuclei per unit area was observed during the course of the experiment.

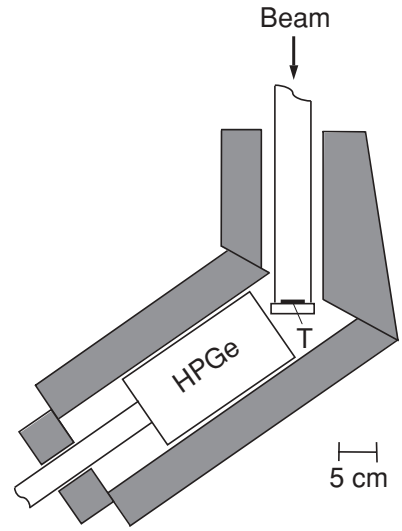

FIG. 4. Schematic setup including beam tube, target ("T"), passive shielding, and γ-ray detector. The detector is located at an angle of $\theta = 55^\circ$ with respect to the beam direction. The lead shield is shown as the grey-shaded area. The detector crystal is surrounded on almost all sides by at least 5 cm of lead.

Prompt γ rays from the $^{17}\text{O}(p,\gamma)^{18}\text{F}$ and $^{18}\text{O}(p,\gamma)^{19}\text{F}$ reactions were detected using a large-volume (582 cm^3) high-purity germanium (HPGe) detector placed at an angle of 55° with respect to the proton beam direction and at a distance of 36 mm between the detector front face and target midpoint. The setup is schematically shown in Fig. 4. The detector crystal was surrounded on almost all sides by at least 5 cm of lead (grey-shaded area). This passive shield reduced unwanted room background between γ-ray energies of 0.6 and 3 MeV by a factor of 48. Energy calibrations were obtained from radioactive sources, background contributions (^{40}K and ^{208}Tl), and well-known decays in the $^{14}\text{N}(p,\gamma)^{15}\text{O}$ reaction [11]. The energy resolution was typically 2.5 keV at $E_\gamma = 1.33$ MeV. Peak efficiency calibrations were established using sources (^{56}Co, ^{60}Co, ^{152}Eu) and decays from the $E_r^{\text{lab}} = 278$ keV resonance in $^{14}\text{N}(p,\gamma)^{15}\text{O}$ [3]. The full-energy peak efficiency amounted to $\approx$1.6% at a γ-ray energy of 1.33 MeV. Since the γ-ray detector was placed in close geometry to the target, coincident summing corrections had to be considered carefully in the efficiency calibrations (see also Sec. IV).

The $^{17}\text{O}(p,\gamma)^{18}\text{F}$ reaction was measured at six laboratory energies, $E_{\text{lab}} = 275$, 300, 325, 400, 450, and 500 keV. At each energy the accumulated charge on the target amounted to 3.2–5.0 C, corresponding to a running time of $\approx$15 h for an average beam intensity of 75 μA. Before and after each run the target was tested by measuring the thick-target yield of the $E_r^{\text{lab}} = 519$ keV resonance. For the strength we obtained a value of $\omega\gamma_{p\gamma} = (1.37 \pm 0.22) \times 10^{-2}$ eV, in agreement with previous values (see Ref. [5] and references therein). As an additional test of our setup to determine reliably absolute cross sections, we measured the resonance strength of the well-known $E_r^{\text{lab}} = 151$ keV resonance in the $^{18}\text{O}(p,\gamma)^{19}\text{F}$ reaction. Our value, $\omega\gamma_{p\gamma} = (9.3 \pm 1.1) \times 10^{-4}$ eV, is in good agreement with previously reported results [5,22,23].

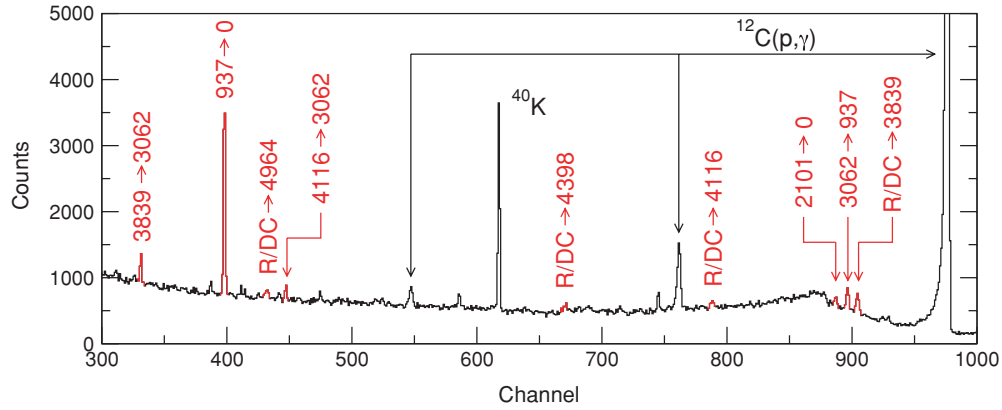

FIG. 5. (Color online) Sample spectrum measured in the $^{17}O(p,\gamma)^{18}F$ reaction at a laboratory energy of $E_{lab} = 400$ keV ($E_{eff}^{c.m.} = 375$ keV). At this energy the direct capture contribution dominates over the resonant component. γ-ray transitions in ^{18}F are marked in red, where "R/DC" refers to the primary transitions. All other peaks arise from environmental and beam-induced background.

IV. ANALYSIS AND RESULTS

A sample γ-ray spectrum is shown in Fig. 5. It was measured at a laboratory energy of $E_{lab} = 400$ keV, where the $^{17}O(p,\gamma)^{18}F$ reaction mainly proceeds via direct capture. In-beam γ-ray transitions in ^{18}F are marked in red. All other peaks arise from room or beam-induced background.

A nonresonant reaction may occur at any location within the thickness of the target. Two essential pieces of information need to be extracted from the data for the estimation of the nonresonant reaction cross section (or S factor): (i) the effective energy and (ii) the total reaction yield.

The effective energy was obtained under the assumption that the cross section varies linearly between $\sigma_1(E)$ and $\sigma_2(E - \Delta)$, where E and Δ are the bombarding energy and the target thickness in energy units, respectively (see Sec. 4.8 of Ref. [3]). This assumption is justified since our ^{17}O target was relatively thin (Sec. III). The cross sections σ_1 and σ_2 were found from the calculated S factor shown as a solid line in Fig. 3. Effective energies computed for different assumptions for σ_1 and σ_2 gave consistent results. The results are listed in Table I. Note that the lowest effective energy in our measurement, $E_{eff}^{c.m.} = 257$ keV, reaches the high-energy boundary of the classical nova Gamow peak ($T = 0.1$–0.4 GK).

The reaction yield is given by the ratio of the total number of ^{18}F compound nuclei formed (or the total number of $^{17}O + p$ reactions that took place) and the total number of incident beam particles (protons), $Y = N_R/N_b$. For in-beam capture γ-ray measurements the quantity N_R can be derived, in principle, in a number of ways. Frequently, it is obtained from the summed and efficiency-corrected intensities of all observed *primary* transitions only. Alternatively, N_R may be obtained from the summed and efficiency-corrected intensities of all observed (secondary and primary) *ground-state* transitions only. A third possibility is the estimation of N_R from *all* observed primary and secondary transitions. We employed the latter method mainly for three reasons: (i) The measured primary transitions were weak compared to the dominant $937 \rightarrow 0$ transition; (ii) using all of the observed intensities should provide a more reliable total yield since it accounts for unobserved transitions that left their fingerprint on the measured intensities, provided that the secondary γ-ray branching ratios are previously known; and (iii) using all of the observed intensities is a prerequisite for proper coincidence summing corrections.

TABLE I. Energies, total cross sections, and S factors for $^{17}O(p,\gamma)^{18}F$.

E^{lab} (keV)	$E_{eff}^{c.m.}$ (keV)	$\sigma(E_{eff}^{c.m.})$ ($\times 10^{-9}$ b)	$S(E_{eff}^{c.m.})$ (keV b)
500.0	469.9 ± 0.5	488 ± 49	17.9 ± 1.8
450.0	422.6 ± 0.5	178 ± 23	10.8 ± 1.4
400.0	375.2 ± 0.5	72.7 ± 8.4	8.13 ± 0.94
325.0	304.3 ± 0.5	18.3 ± 3.1	6.7 ± 1.1
300.0	280.7 ± 0.5	10.8 ± 1.9	6.5 ± 1.2
275.0	257.1 ± 0.5	6.6 ± 1.5	7.0 ± 1.5

Recall that our γ-ray detector was positioned in close proximity to the target. Consequently, coincidence summing corrections have to be considered carefully. The corrections were performed numerically using a computer code, LENASUM, based on the matrix formalism described in Ref. [24]. The code uses as input the intensities of all observed (primary and secondary) γ-ray transitions, as described previously. Required total efficiency values were computed using the Monte Carlo code GEANT4 [25] and were normalized to the total efficiency measured (using the sum-peak method [3]) with a ^{60}Co source. Peak efficiency values were also obtained using GEANT4 to aid with the interpolation of efficiencies between measured values. The entire experimental setup, including detector housing, contact pin, shielding, target holder, and chamber, was included in the simulations. The γ-ray branching ratios for the secondary transitions are well known for ^{18}F and were adopted from Table 18.25 of Tilley *et al.* [11]. For example, for the dominant $937 \rightarrow 0$ γ-ray transition, coincident summing corrections amounted to 13–17%, depending on the proton bombarding energy. Our measured intensities for all observed primary and secondary γ-ray transitions in ^{18}F are listed in Table II. At the bottom of the table, we list for each bombarding energy the total number of reactions that occurred, properly

TABLE II. Measured γ-ray intensities and total yields in $^{17}O(p,\gamma)^{18}F$.

Transition[a] $E_f \rightarrow E_i$	Intensity[b]					
	275 keV	300 keV	325 keV	400 keV	450 keV	500 keV
$937 \rightarrow 0$	456(61)	689(51)	1202(95)	5820(109)	11700(179)	30221(218)
$1042 \rightarrow 0$					229(107)	522(74)
$1081 \rightarrow 0$				144(73)	365(123)	525(75)
$2101 \rightarrow 0$				107(71)		522(117)
$2523 \rightarrow 0$				108(30)	344(42)	1031(68)
$3062 \rightarrow 0$			59(27)	243(40)	479(42)	1003(69)
$3839 \rightarrow 0$		30(13)	47(27)	287(42)	472(50)	1374(78)
$1121 \rightarrow 937$						3144(349)
$2101 \rightarrow 937$					136(111)	544(87)
$2523 \rightarrow 937$						534(104)
$3062 \rightarrow 937$			159(40)	811(71)		3707(139)
$3791 \rightarrow 2101$						1325(99)
$3791 \rightarrow 3062$						1048(133)
$3839 \rightarrow 937$					108(28)	418(59)
$3839 \rightarrow 3062$			133(64)	655(79)	1337(125)	3981(137)
$4116 \rightarrow 3062$			71(55)	373(76)	686(110)	1076(117)
$4398 \rightarrow 937$						91(46)
$R \rightarrow 937$	37(11)	117(23)	241(48)	959(71)		5919(137)
$R \rightarrow 1121$				186(50)	334(48)	
$R \rightarrow 2101$						86(42)
$R \rightarrow 2523$				148(33)	382(52)	1047(79)
$R \rightarrow 3062$	18(10)	45(15)	76(31)	305(46)	437(41)	922(70)
$R \rightarrow 3358$						196(49)
$R \rightarrow 3791$				105(55)		1531(91)
$R \rightarrow 3839$		122(29)	196(44)	807(75)	1654(159)	5194(134)
$R \rightarrow 4116$				289(69)	437(129)	973(115)
$R \rightarrow 4398$				241(57)		370(105)
$R \rightarrow 4652$						341(95)
$R \rightarrow 4753$						153(66)
$R \rightarrow 4860$						110(84)
$R \rightarrow 4964$		137(46)		395(86)	405(124)	544(102)
Total[c]:	45287 (±20%)	62130 (±15%)	100213 (±14%)	470054 (±7%)	947079 (±9%)	2352190 (±4%)
Charge (C)[d]:	5.00	4.09	3.78	4.23	3.62	3.21

[a]Transition from initial to final state. Energies are in units of keV. The label R refers to primary transitions.
[b]Measured raw intensities at six laboratory bombarding energies. The values listed are neither corrected for peak efficiencies nor for coincidence summing.
[c]Total number of reactions that occurred, equal to the total number of ^{18}F nuclei produced. The values listed are corrected for both peak efficiencies and coincidence summing.
[d]Total accumulated charge in Coulomb. Division by the elementary charge gives the total number of incident protons.

corrected both for peak efficiencies and coincidence summing. The total accumulated charge on target is also given.

Angular correlation effects are expected to be negligible in our measurement. The two broad resonances at $E_r^{\rm lab} = 589$ keV ($J^\pi = 3^+$) and $E_r^{\rm lab} = 716$ keV ($J^\pi = 2^+$) are formed via s waves and thus have an isotropic emission pattern. They also do not interfere in the total cross section since they have different J^π values. Furthermore, all of the strong direct capture transitions in $^{17}O + p$ proceed from incoming p or f waves into s or d final states. These direct capture angular distributions are of the form $W(\theta) = 1 + a_2 P_2(\cos\theta)$, where the P_2 term is zero near our chosen detector angle of $\theta = 55^\circ$. Similarly, interference of direct capture amplitudes with different incoming orbital angular momenta gives rise to a correlation of the form $W(\theta) = a_2 P_2(\cos\theta)$ and thus will not produce anisotropies near $\theta = 55^\circ$. As already pointed out, the broad resonances at $E_r^{\rm lab} = 589$ and 716 keV are formed via s waves ($\ell_r = 0$) and therefore do not interfere in the *total* cross section with the main direct capture transitions, which proceed via $\ell_i = 1$ or 3 waves. In principle, the resonance-direct capture interference can give rise to a P_1 term. However, the resonances decay mainly via $M1$ transitions [26] for which the Racah coefficient in the angular correlation expression (Eq. (A.38) in Ref. [13]) disappears. These arguments apply only to the main resonant and direct capture transitions. Weak transitions may indeed exhibit anisotropies. However, we note that the γ-ray decay strength is rather fragmented and thus small anisotropies in some minor transitions will have only

a negligible effect on the total cross section. In addition, our γ-ray detector was located in close geometry to the target, which further weakens any angular correlation effects.

The cross section at the effective energy, $\sigma(E_{\rm eff})$, is obtained from the expression [3]

$$\sigma(E_{\rm eff}) = \frac{Y(E)}{n} = Y(E)\frac{\epsilon_{\rm eff}(E)}{\Delta(E)}, \qquad (2)$$

with Y the reaction yield at bombarding energy E, n the number of ^{17}O target nuclei per unit area, $\epsilon_{\rm eff}$ the effective stopping power, and Δ the target thickness in energy units (see Sec. III). All kinematic quantities in the above expression are in the center-of-mass system. The center-of-mass effective stopping power for our ^{17}O target is given by Bragg's rule

$$\epsilon_{\rm eff} = \frac{N(\rm O)}{N(^{17}\rm O)}\epsilon(\rm O) + \frac{N(\rm Ta)}{N(^{17}\rm O)}\epsilon(\rm Ta), \qquad (3)$$

where $N(\rm O) = N(^{16}\rm O) + N(^{17}\rm O) + N(^{18}\rm O)$ (assuming that the oxygen isotopes have the same stopping power). For example, at a laboratory energy of $E = 519$ keV we obtain $\epsilon_{\rm eff} = (19.1 \pm 0.7) \times 10^{-15}$ eV cm^2 in the center of mass. The ratios of number densities N_i are calculated from the target stoichiometry of O:Ta = 5:2 and the known ^{17}O enrichment (Sec. III). Stopping powers $\epsilon_i^{\rm lab}$ are computed using the code SRIM [27] and are converted to the center-of-mass system. At a laboratory energy of 519 keV we find for the number of ^{17}O target nuclei per unit area a value of $n = \Delta(E)/\epsilon_{\rm eff}(E) = (2.34 \pm 0.13) \times 10^{17}$ cm^{-2}. The resulting cross sections and corresponding S factors are listed in Table I.

The measured total S factors from the present work are displayed in Fig. 6 as red data points together with previous results. In fact, this plot is the same as Fig. 3, except that the S-factor scale is linear instead of logarithmic and that the present data are included. Our lowest data point at $E_r^{\rm c.m.} = 257$ keV appears at the high-energy boundary of the classical nova Gamow peak region (for $T = 0.1$–0.4 GK). It is apparent that our total S-factor data agree with the prediction of Fox *et al.* [5], which is shown as a solid line. This is important since it justifies the method applied in Fox *et al.* [5] of estimating direct capture S factors from single-particle potential model calculations and experimental spectroscopic factors (see Sec. II). We note again that this particular method has been applied in thermonuclear rate calculations of numerous other reactions, but has rarely been tested before.

Our measured total S factors can be used to extract the direct capture contribution. To this end, we subtract the calculated S factor arising from the two broad resonances at $E_r^{\rm c.m.} = 557$ and 677 keV (see Sec. II and dashed line in Fig. 6) from our measured total S factor. The extracted direct capture S factor is nearly energy independent and is well described by a constant S factor below $E_{\rm c.m.} = 500$ keV

$$S_{\rm DC}(E) = 4.6\ \text{keVb}\ (\pm 23\%), \qquad (4)$$

where the quoted uncertainty accounts for the uncertainties of the $E_r^{\rm c.m.} = 557$ and 677 keV resonance parameters. This result deviates from the predicted direct capture S factor of Fox *et al.* [5] (dashed horizontal line in Fig. 6) by only 20% near the middle of the classical nova Gamow peak

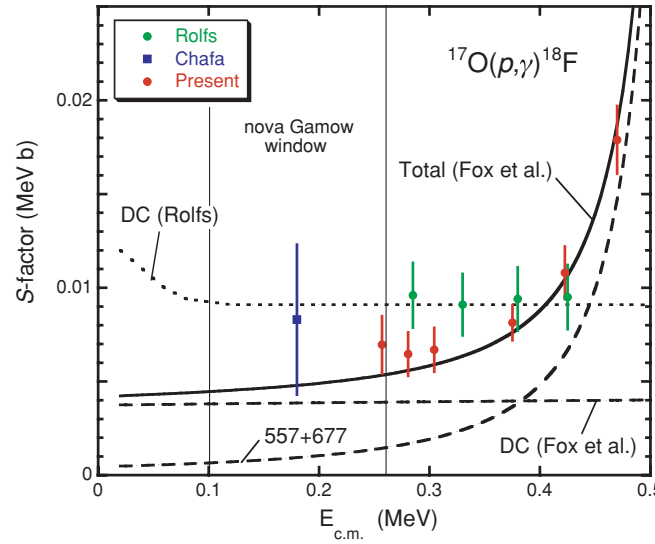

FIG. 6. (Color online) Same as Fig. 3, except that our measured S factors are included as full red circles and the vertical scale is linear instead of logarithmic. All data points refer to measured *total* S factors. Our lowest data point at $E_r^{\rm c.m.} = 257$ keV appears at the high-energy boundary of the classical nova Gamow peak region (for $T = 0.1$–0.4 GK). Our extracted direct capture S factor agrees within uncertainties with the prediction of Fox *et al.* [5] (horizontal dashed line), but disagrees with the result of Rolfs [13] (dotted line) by a factor of $\approx$2. Note that the solid line is not a fit to our data, but represents the total S factor predicted by Fox *et al.* [5].

($\approx$180 keV). We improved the uncertainty of the direct capture S factor from an assumed value of $\pm$50% in Ref. [5] to an experimental value of $\pm$23% in the present work. It is also apparent that our extracted direct capture S factor disagrees with the result of Rolfs [13] (dotted line in Fig. 6) by a factor of $\approx$2 near an energy of 180 keV. As already pointed out in Sec. II, the uncertainty on the data point from Ref. [7] is too large to be of any significance. New thermonuclear reaction rates for $^{17}O(p,\gamma)^{18}F$ will be published elsewhere.

V. SUMMARY AND CONCLUSION

The $^{17}O(p,\gamma)^{18}F$ reaction represents a rare example for a situation where, for a given range of temperatures (here $T = 0.1$–0.4 GK), the total thermonuclear reaction rates are dominated by the direct capture process despite the fact that a narrow resonance is located well inside the Gamow peak. In this work we reported on a measurement of the total capture S factor at low bombarding energies between $E_{\rm lab} = 275$ and 500 keV. The lowest energy measured, corresponding to an effective energy of $E_{\rm eff}^{\rm c.m.} = 257$ keV, is located at the high-energy boundary of the classical nova Gamow peak ($T = 0.1$–0.4 GK). We extract from our data a new direct capture S factor, which agrees with the prediction of Fox *et al.* [5] within 20% near the middle of the classical nova Gamow peak ($\approx$180 keV). However, our extracted direct capture S factor disagrees with the results of Rolfs [13] by a factor of $\approx$2 near an energy of 180 keV. We also achieved a significant reduction in

the direct capture S factor uncertainty, from $\pm 50\%$ in Ref. [5] to $\pm 23\%$ in the present work. New thermonuclear reaction rates for $^{17}\mathrm{O}(p,\gamma)^{18}\mathrm{F}$ will be presented elsewhere.

ACKNOWLEDGMENTS

This work was supported in part by the US Department of Energy under Contract No. DE-FG02-97ER41041.

[1] S. Starrfield, C. Iliadis, and W. R. Hix, in *Thermonuclear Processes, Classical Novae* (2nd ed.) edited by M. F. Bode and A. Evans (Cambridge University Press, Cambridge, England, 2008).

[2] C. Fox, C. Iliadis, A. E. Champagne, A. Coc, J. José, R. Longland, J. Newton, J. Pollanen, and R. Runkle, Phys. Rev. Lett. **93**, 081102 (2004).

[3] C. Iliadis, *Nuclear Physics of Stars* (Wiley-VCH, Weinheim, 2007).

[4] C. Angulo *et al.*, Nucl. Phys. A **656**, 3 (1999).

[5] C. Fox, C. Iliadis, A. E. Champagne, R. P. Fitzgerald, R. Longland, J. Newton, J. Pollanen, and R. Runkle, Phys. Rev. C **71**, 055801 (2005).

[6] A. Chafa *et al.*, Phys. Rev. Lett. **95**, 031101 (2005).

[7] A. Chafa *et al.*, Phys. Rev. C **75**, 035810 (2007).

[8] A. Chafa *et al.*, Phys. Rev. Lett. **96**, 019902(E) (2006).

[9] J. R. Newton, C. Iliadis, A. E. Champagne, R. Longland, and C. Ugalde, Phys. Rev. C **75**, 055808 (2007).

[10] B. H. Moazen *et al.*, Phys. Rev. C **75**, 065801 (2007).

[11] D. R. Tilley, H. R. Weller, C. M. Cheves, and R. M. Chasteler, Nucl. Phys. A **595**, 1 (1995).

[12] G. Audi, A. H. Wapstra, and C. Thibault, Nucl. Phys. A **729**, 337 (2003).

[13] C. Rolfs, Nucl. Phys. A **217**, 29 (1973).

[14] C. Iliadis and M. Wiescher, Phys. Rev. C **69**, 064305 (2004).

[15] C. Iliadis, J. D'Auria, S. Starrfield, W. J. Thompson, and M. Wiescher, Astrophys. J. Suppl. **134**, 151 (2001).

[16] C. Iliadis, C. Angulo, P. Descouvemont, M. Lugaro, and P. Mohr, Phys. Rev. C **77**, 045802 (2008).

[17] L. M. Polsky, C. H. Holbrow, and R. Middleton, Phys. Rev. **186**, 966 (1969).

[18] V. Landre, P. Aguer, G. Bogaert, A. Lefebvre, J. P. Thibaud, S. Fortier, J. M. Maison, and J. Vernotte, Phys. Rev. C **40**, 1972 (1989).

[19] P. M. Endt, Nucl. Phys. A **521**, 1 (1990).

[20] D. Phillips and J. P. S. Pringle, Nucl. Instrum. Methods **135**, 389 (1976).

[21] D. A. Vermilyea, Acta Metall. **1**, 282 (1953).

[22] M. Wiescher *et al.*, Nucl. Phys. A **349**, 165 (1980).

[23] R. B. Vogelaar, T. R. Wang, S. E. Kellogg, and R. W. Kavanagh, Phys. Rev. C **42**, 753 (1990).

[24] T. Semkow, G. Mehmood, P. Parekh, and M. Virgil, Nucl. Instrum. Methods A **290**, 437 (1990).

[25] S. Agostinelli *et al.*, Nucl. Instrum. Methods A **506**, 250 (2003); we used the low-energy extensions of GEANT4 according to www.ge.infn.it/geant4/lowE/index.html.

[26] C. Rolfs *et al.*, Nucl. Phys. A **199**, 328 (1973).

[27] J. F. Ziegler and J. P. Biersack, computer program SRIM (2003).